International Journal of Design & Nature and Ecodynamics
Vol. 19, No. 6, December, 2024, pp. 1887-1899
Journal homepage: http://iieta.org/journals/ijdne

Groundwater Remediation for Irrigation at Al-Raaed Station Using Banana Peel-Derived Activated Carbon

Omayma N. Mohammed*, Hayder M. Abdulhameed

Environmental Department, Engineering College, Baghdad University, Baghdad 10001, Iraq

Corresponding Author Email: omaima.nezar2111p@coeng.uobaghdad.edu.iq

https://doi.org/10.18280/ijdne.190605

Received: 23 October 2024
Revised: 18 November 2024
Accepted: 29 November 2024
Available online: 27 December 2024

Keywords:
groundwater, adsorption, batch mode, irrigation, activated carbon, banana peels, Al-Raaed station, banana peels activated carbon

ABSTRACT

This study aims to evaluate the efficiency of banana peel-derived activated carbon (BPAC) in removing cations, ions, and TDS from groundwater at Al-Raaed station for safe irrigation use. Al-Raaed station in Abu Ghraib, which is linked with the Ministry of Water Resources, relies on groundwater for irrigation. This research aims to tackle the issue of elevated groundwater salinity and associated pollutants (eliminate cations, ions, and total dissolved solids (TDS)) from groundwater (GW) in the wells, ensuring that groundwater treatment adheres to and is aligned with the guidelines of the Food and Agriculture Organization (FAO), and promoting the use of treated groundwater for irrigation and agricultural purposes by local farmers. The goal is to make the groundwater suitable for irrigation by implementing adsorption technology to reduce the concentration of pollutants. Banana peel-derived activated carbon (BPAC) is ready for use as an adsorbent. The chemical composition of the materials was examined using XRD, SEM, and FTIR spectroscopy. For optimal conditions to extract groundwater suited for irrigation, the adsorption process's four parameters—dosage, duration, agitation speed, and pH—were examined. When planning water management for sustainable productivity, it is essential to have a firm grasp of the topic of irrigation water quality. Key quality indicators such as pH, EC, total dissolved solid (TDS), cations, and anions were measured in laboratory water samples. The overarching goal of this investigation was to use treated groundwater for irrigating crops. The most effective clearance rates were 76% for Mg and 94% for K, occurring at a dosage of 2.5 g with an optimal duration of sixty minutes. For Ca, Na, and Cl, the removal efficiencies were 53%, 72%, and 57%, respectively. A removal efficiency of 47% for Ca, 43% for SO_4, and 53% for Na can be achieved at an agitation speed of 150 rpm. Optimal acidity is at pH 5, with removal efficiencies of 83% for Mg, 52% for SO_4, 94% for K, and 47% for NO_3. The groundwater emerging from remediation by adsorption is suitability to FAO guidelines promoting the use of treated groundwater for irrigation and agricultural purposes by local farmers. The principles apply FAO guidelines to evaluating groundwater for irrigation for chemical elements such dissolved salts, sodium concentration, and harmful ions.

1. INTRODUCTION

Groundwater has been a vital resource for human water needs since prehistoric times. Pure, high-quality groundwater is not polluted and is rich in beneficial microbes and organic substances. On the flip side, groundwater may contain a variety of cations and anions due to salinity caused by dissolved salts. More than half of the world's population relies on underground sources for its drinking water [1].

One of the most valuable resources our country has is groundwater, which is found in underground aquifers. About 37% of the water that public water departments in counties and cities get for homes and businesses comes from underground sources.

Wells lose their ability to access groundwater when the groundwater table is lowered due to excessive pumping, leading to increased costs. A decrease in the water table causes an increase in the energy required to pump water to the surface. The expense of using such a well might be too high in the worst-case scenario [2].

Containers on land or in subterranean storage tanks are common storage places for hazardous chemicals. Soil and groundwater contamination might result from leaks in these storage containers and tanks. Fuel from petrol stations, including both gasoline and diesel, as well as solvents, heavy metals, and pesticides, commonly contaminates soil and groundwater.

Landfills, industrial-discharge lagoons, leaking gasoline storage tanks, cesspools, septic tanks, pesticides, fertilizers, and manure applied to agricultural areas are some of the sources of chemicals that can be introduced to groundwater in this manner.

A variety of human-generated contaminants cause groundwater pollution. These include the overuse of pesticides,

herbicides, and fertilizers; poorly managed landfills; leaking fuel and chemical tanks; industrial chemical accidents; and the drainage of household chemicals. The contamination is exacerbating the worldwide problem of insufficient access to potable water. Due to the shortage of clean groundwater supplies and safe drinking water, water treatment is recommended before use by various international and national bodies, including the World Health Organization [1].

Groundwater contamination can adversely impact the quality of land and forests. Contaminated groundwater can result in soil contamination and deterioration of land quality. For example, in many agricultural areas in arid climates, high groundwater salinity is one of the key factors influencing soil salinization [3]. Soluble salts and other pollutants, including hazardous metals, can build in the root zone, adversely impacting vegetation growth. Contaminants in groundwater can be conveyed through interactions between surface water and groundwater, resulting in a decline in surface water quality.

Groundwater contamination can potentially impact human health by affecting the food production chain. Irrigation utilizing groundwater contaminated by heavy metals and wastewater containing persistent pollutants can lead to the accumulation of hazardous components in cereals and vegetables, posing health concerns to humans [4].

Research using hardness as a proxy for water quality has been ongoing for some time. Hard water causes a lot of problems in homes and businesses. The hardness of water is primarily caused by cations such as magnesium and calcium and, to a lesser degree, by bivalent and trivalent metals like aluminum and iron. To keep up with the ever-increasing demand for soft water of excellent quality, efficient and inexpensive technology is urgently required [5]. The salinity of groundwater is a problem all throughout the world. Consequently, it endangers human health, lowers agricultural profits and yields, degrades arable land, increases the cost of maintaining infrastructure and running industrial activities, and changes or destroys ecosystems. How the groundwater is utilized to meet the water demand for these processes and activities, as well as its salt content, determines all of this. Results from the research of Weert, Gun, and Reckman indicate [5].

Humanity is currently tackling the extremely challenging subject of a potential worldwide water scarcity. An increase in water consumption is a direct result of the correlation between a growing global population and the subsequent boom in industrialization, which is driven by the increased demand for manufactured goods. Jasim et al. [6] asserted that polluted water endangers human existence and civilization's advancement.

Al Haider et al. [7] reported that a permeable reactive barrier (PRB) made of activated carbon from banana peels (BPAC) was investigated as a potential method for removing copper (Cu^{+2}) from the polluted groundwater. By using phosphoric acid as a soaking agent, the banana peels were chemically activated to produce the activated carbon. Batch experiments were used to examine the effects of several parameters, such as the pH of the starting solution, the speed of the agitation, the initial quantity of copper, the contacting length, and the dosage of the sorbent. The variables with the most significant impact on copper removal efficacy (96%) are as follows: 1 mg/100 ml, 40 minutes at 250 rpm, and 50 mg/l. Batch investigational data on Cu^{+2} ion sorption was analyzed using the Freundlich and Langmuir isotherm models.

The results point to the Langmuir model as a possible explanation for the Cu^{+2} sorption onto BPAC. The one-dimensional (1D) copper transport equations under equilibrium conditions have been solved by our group using the finite element method in COMSOL Multiphysics 3.5a. Both the actual results and the expected results (COMSOL solution) indicate that the PRB is a crucial component in stopping the flow of the copper plume. The impressive level of agreement between predicted (theoretical) and observed results, along with an RMSE of less than 0.1%, proves that these methods are practical and valuable tools for studying copper transport pathways [7].

Removing anions, total dissolved solids (TDS), and chloride ions is necessary to make groundwater (GW) appropriate for irrigation, according to Raheem and Abdul-Hameed [8]. In order to bring the experimental results into practice, the scientists suggest adopting adsorption technology to reduce the concentration of pollutants in GW. A banana-derived graphene adsorbent (BPAC) has the potential to be flash-synthesized as FG. A synthetic method for producing FG has been developed, which involves the use of an electro-flash reactor to rapidly transform BPAC into graphene. With each cycle of 8-10 shocks administered by the reactor's manual circuit break, 5 grams of FG are produced from BPAC. To clean up the GW samples, in batch mode adsorption, one variable (such as agitation speed, pH value, contact period, or FG dosage) is changed per trial while keeping the others constant. The assessment of (FG) is conducted to analyze the chemical composition of the materials via XRD, SEM, and an FTIR spectrometer. To increase the adsorption capacity, a structure was developed with large interior pores. This structure not only offers a high adsorption capacity but also provides a significant surface area. It is effective in increasing the concentrations of TDS, SO_4, NO_3, and Cr^6 in the irrigation water until it meets the requirements set by Iraq and the FAO.

The possible detrimental effects of pharmaceutical pollutants on human health, the environment, and the economy are causing pharmaceutical pollutants to get increasing attention [9]. Cleaning up polluted areas by adsorption is one cost-effective option. This work employed activated carbon derived from banana peels, an agro-industrial waste product, to extract amoxicillin and carbamazepine from various water matrices. In order to carbonize the phosphoric acid-activated carbon, temperatures of 350°C, 450°C, and 550°C were employed. Scanning electron microscopy (SEM) analyses of banana peel activated carbon (BPAC) samples showed a heterogeneous, semi-regular morphology characterized by many pores of varying sizes and shapes. According to Boehm titration, the activation by H_3PO_4 led to an increase of 0.711 mmol/g of acidic groups. After the pollutant molecules were effectively adsorbed and activated, the spectroscopic features of the BPAC surface changed dramatically, as seen by the distinct FTIR peaks. A pHpzc value of 5.005 was determined for the BPAC. Assessment with the SBET instrument. Following activation, the surface area grew substantially to 911.59 m^2/g. In a world where all is ideal, with a pollutant mixture of 25 mg/L, a temperature of 25°C, and a dosage of 1.2 g/L of materials, saturation lasts 120 minutes at a pH level of 5. The residual value is negligible when Langmuir is utilized, even though Freundlich provides a somewhat better fit. As the sum of squares (SSE) demonstrated, the results were more consistent with the pseudo-second-order kinetic. The current research demonstrated that agricultural and industrial effluents might be utilized to eliminate organic micropollutants through the application of ecologically sound

disposal techniques [9].

Traditional methods of waste management, such as incineration or landfilling, result in environmental degradation and the depletion of biomass, a resource that may be utilized more effectively. Waste products from agricultural crop production and harvesting can be utilized in large quantities for wastewater treatment. Among these materials are straw, stones, and shells. In the first case, it is used directly as an adsorbent after ambient drying and grinding; in the second, it forms part of modified bio-based sorbents; and in the third, it becomes a component in the carbonization process that produces activated carbon adsorbents. The feasibility of removing residual compounds from complex matrices is not well understood. Researchers must conduct more hands-on research into environmental samples and other natural matrices without spiking target compounds. This is true even though there is a mountain of literature devoted to finding solutions for the problems caused by metals, metalloids, dyes, pesticides, and other emerging contaminants. The phase inversion method was first used to create hybrid cellulose acetate (CA) membranes, as stated by Ali et al. [10]. Membranes composed of activated carbon derived from sunflower seed shells (SFAC) were immersed in a polymer casting solution that contained CA to purify polluted water. Phosphoric acid was employed as the activator. The carbonization temperatures of the activated carbons SFAC7, SFAC8, and SFAC9, which are generated using an agent in a 3:1 (wt.) ratio, differ. The SBET sample with the highest surface area was the SFAC9 sample (786.62 m^2 g^{-1}). A pore radius of r-and a total pore volume of 8.7694 lbs (VT) 4.00226 nanometers. An exploration of several beginning concentrations (5-20 mg/L), SFAC dosages (0.1-0.5), and their respective effects. Contact time (0.5-24 h) and pH (2-12 h) were among the parameters examined. The data indicated that 0.1% of the CA was SFAC9, with a clearance rate of 84.67% under particular conditions. This rendered it the superior membrane in terms of crystal violet (CV) dye elimination and superb ecological condition. We employed a battery of techniques to flush the CA (SFAC9 0.1%) membrane of dye. The adsorption isotherms were determined using the Freundlich model. Additional evidence for chemisorption has been found in kinetic investigations in the form of pseudo second.

According to Naser and Abdul-Hameed [11], heavy metal ion pollution is common in industries such as electroplating, metal processing, and mining. The toxic waste that results from the increased discharge of water polluted with copper (Cu II) is a major concern for the environment around the world. A more practical method for heavy metal removal is adsorption, which has a number of benefits such as simplicity, repeatability, and sensitivity, as well as economic ones like efficacy. This study examined the capacity of an adsorbent derived from orange peel (OP) to extract copper (II) from solutions in water.

Additionally, the effects of changes in solution pH, initial Cu (II) concentration, adsorbent dosage, and contact time on the sorbent material's effectiveness were identified. It was additionally studied adsorption kinetics and adsorption equilibrium isotherm to have a better understanding of adsorption processes [11].

Table 1 shows cations, anions and other measurements recommended for characterizing irrigation.

Many research has been utilized Banna peels for removing heavy metals, and organic pollutants. This study will be investigated for removing ions from ground water and in other words use a new effective adsorbent for removing contaminates from groundwater.

Table 1. Cations, anions and other measurements recommended for characterizing irrigation [12]

Cations	Anions	Others
Calcium (Ca^{+2})	Chloride (Cl^-)	Total dissolved solids (TDS)
Magnesium (Mg^{2+})	Nitrate (NO^-)	Electrical conductivity (EC)
Sodium (Na^+)	Sulphate (SO_4^{2-})	Acidity/Alkalinity
Potassium (K^+)	Bicarbonate (HCO_3^-)	

The purpose of this article is to examine contemporary developments in activated carbon as well as its uses and relevant applications, including its effects on areas like contamination removal and detection. Evidence from the adsorption mechanism study points to a chemical basis for the adsorption process, with ion exchange playing a key role. In addition, this article synthesized activated carbon from banana peels and employed it as an adsorbent material to study the removal effectiveness for contaminants in ground water.

2. LITERATURE REVIEW

2.1 Adsorption

One effective and tried-and-true method for cleaning wastewater from houses and companies is adsorption. When it comes to adsorbents, activated carbon is widely recognized as an effective adsorbent. A network of linked macro-, meso-, and micro-pores characterizes the porous structure of activated carbon in either its powder or granular form. These pores are great in attracting organic substances due to their large surface area. The kind of bonding mechanisms and the amount and intensity of adsorption are determined by the adsorbate's chemical properties, such as its solubility, ionic nature, and functional groups, in conjunction with the activated carbon's surface chemistry [13, 14]. According to Jasim et al. [15], adsorption is the most effective method for eliminating contaminants. Activated carbon's adsorption capabilities have made it a crucial part of water treatment systems all over the world. Although its once-enticing low price has turned it into an unappealing option for large-scale processes and industries, it has lately transformed into a cost-effective adsorbent [16].

Making activated carbons from banana rinds is the focus of this research. The banana peels were pyrolyzed for one hour at 700°C in three different environments: open air (O_2-BP), nitrogen gas (N_2-BP), and a mixture of nitrogen gas and water steam (N_2+H_2O-BP) that was heated to 60-70°C. The adsorption process was fine-tuned by adjusting a number of factors, including pH (ranging from 4 to 10), contact period, and initial concentration of metal ions. The ideal pH for the adsorption of arsenate (III) was 7. The process of adsorption of the arsenate ion took two hours to reach equilibrium. Since the experimental data were better matched to the Langmuir equation, which had a high coefficient of determination value (R2 = 0.9934), the Freundlich and Langmuir isotherms were used to calculate the adsorption isotherms. Using a rate constant of 0.0111 g/(mg.min), the experimental data was well-fit by the pseudo second-order kinetic model. The

physiosorption mechanism was followed by the spontaneous adsorption of As(III) on banana peels. For all starting concentrations of As(III) ions, the value of the separation parameters (RL) was determined to be between 0 and 1, indicating excellent adsorption into banana peels [17].

Adsorption is an economical method for cleaning up polluted areas. Therefore, this study synthesized activated carbon from banana peels, an agro-industrial waste product, to remove amoxicillin and carbamazepine from various water matrices. At temperatures of 350°C, 450°C, and 550°C, the carbon that had been chemically activated by phosphoric acid (H_3PO_4) was carbonized. Once the pollutant molecules were activated and adsorbed onto the BPAC surface, FTIR detected new peaks, indicating that the surface's spectroscopic properties had changed significantly. It was determined that BPAC has a pHpzc = 5.005. Following activation, the SBET surface area jumped to 911.59 m^2/g. An ideal set of circumstances would have been 25°C, 1.2 g/L of materials, 120 min of saturation, 25 mg/L of pollutants, and a pH of 5. With a low residual sum of squares (SSE) and data that were better fitted to the pseudo-second-order kinetic, Langmuir shows a somewhat better fit than Freundlich. In addition, over the seven cycles, BPAC was effectively tested for its ability to remove pharmaceuticals from Milli Q water, lake water, and wastewater. The current study's findings demonstrated the possibility of using agro-industrial waste to remove organic micropollutants, all while demonstrating sustainable waste management practices [9].

2.2 Factors affecting adsorption

In various operating conditions, including pH, adsorbent dose, and contact time, a variety of materials have been studied, including synthetic, hybrid, and naturally occurring adsorbents. To determine operating parameters for efficient La adsorption, however, further work is needed to thoroughly review the abundance of studies. Here, the effect of operating conditions on the adsorption process of various materials is discussed.

Several variables impacted the adsorption process, including [18]:

1. The adsorbent's particle size: When the size of the holes is compared to that of the molecule, it becomes clear that very small pores will not allow very large molecules to pass through. Pores that are too small will not allow large molecules to pass. Assimilation will be more of a challenge as a result. Adsorbent internal diffusion and mass transfer are hindered by particles with small diameters. Because of this, approaching mean equilibrium and the maximum adsorption capacity is a breeze.

Müller [19] stated that the adsorption of albumin-bonded bilirubin on activated carbon with different pore sizes and distributions spanning the micropore and mesopore range was the subject of a comprehensive examination. The findings show that when the particle size decreases, efficiency increases. Bilirubin sorption was most effective with activated carbon that had a large BET surface area, a benzene mesopore volume of around 0.18 $cm^3\ g^{-1}$, and an average particle diameter of about 82 lm. This highly activated carbon adsorbed 58% of the initially accessible bilirubin within 1 hour of adsorption in batch testing. A diffusion coefficient of about 0.60×10^{-10} $cm^2\ s^{-1}$ for bilirubin adsorption employing this highly activated carbon was produced using an intraparticle mass transfer model of sorptive absorption from a stirred solution of confined volume in spherical particles. Another potential outcome of the adsorption process is the separation of albumin and bilirubin. Further research into the bilirubin sorption mechanism from B-HSA solutions is necessary for this reason.

The information gathered from this study can help clarify both the overall adsorption process and the details of albumin-bonded toxin adsorption in porous materials. This, in turn, can help with the design of toxin adsorbers that depend on size-dependent adsorption properties and pressure drops within the packed bed [19].

2. Contact time: Even with larger equipment, a longer residence period will provide a more comprehensive adsorption treatment.

3. Adsorbates' solubility in wastewater: It is easier to extract substances from water that aren't extremely soluble. Similar considerations apply to non-polar chemicals; they are more amenable to adsorption than polar substances, which exhibit a substantially larger attraction to water.

4. A material that contains a higher concentration of carbon atoms is more likely to be adsorbed since it is less polar.

5. The degree of ionization of the adsorbed molecule: Adsorption is less likely to occur with ionized molecules compared to neutral molecules.

Lastly, the adsorbate's ionization level is affected by the pH. Because of this, its efficacy will be altered.

3. RESEARCH METHODOLOGY

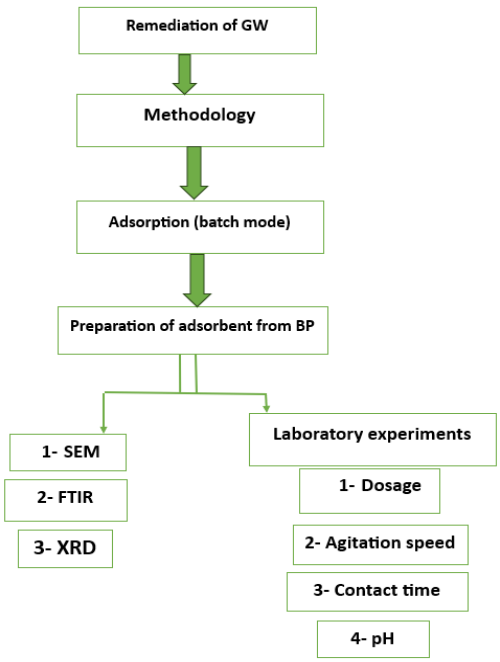

Figure 1. The flowchart of the experimental work

At Al-Raaed station in Abu Ghraib affiliated to the Ministry of Water Resources, there are high levels of pollution and extreme salinity in groundwater. There are well in location, it stays away at 25 m. Due to the Ministry's need to convert well water into water suitable for irrigation, so a system has been used to treat it to use it for irrigation purposes by adsorption system and comparison of results with the Food and Agricultural Organization (FAO). Figure 1 shows the procedure of the experimental work.

3.1 Materials

The materials were used in this paper as the following described in Table 2.

In Table 3, it is shown the equipment used in the experiment.

Table 2. The material was used in this research

Name	Chemical Formula	Molecular Weight (gm/mol)	Manufacturing Company
Hydrochloric acid	HCL	136.29	China
Zinc chloride	$ZnCl_2$	36.46	China
Banana peels	-		Locally available

Table 3. The laboratory equipment

Name	Manufacturing Company
Digital pH meter	China
Platform shaker	Julabo Labrotechnik Gmbh, Germany
Furnace	SAFTHERM, China
Mixer grinder	China
Glass wares	China
Conical flask	China
pipette	China

Raw banana peel was sourced from a nearby juice shop. Rinsing the banana peel with distilled water removed any leftover dust particles. After the peel had dried completely in the sun, it was baked at 105°C for 24 hours to extract any remaining moisture. After drying, the peel was ground into a powder using an attrition mill. The banana peel powder was made by sieving the fruit (Figure 2) [20]. For the next step, the powdered banana peel was carbonized in a furnace set at 500°C for an hour. After being immersed in a zink chloride ($ZnCl_2$) solution for 14 hours at a 3:1 (w/w) impregnation ratio in 10 ml of aquades, the carbonized material (char) was dehydrated in an oven set at 110°C for 6 hours. Zinc chloride was added in (3:1) (w/w) and 98% in concentrations. The ACBP was utilized in 10.5 g in the experiment and the particle size was (1.7 µm).

Figure 2. Stages of burning banana peels to adsorbent

After that, the sample was physically activated by heating it in a furnace set at 700°C for an hour. Once cooled, the activated carbon (AC) was rinsed with 0.2 N HCl to dissolve and remove any remaining ash. Then, it was washed again with hot distilled water until the pH reached 7.0. The activated carbons were then oven-dried to a consistent weight at 110°C [21]. Figure 3 expresses the flowchart of the synthesis of the ACBP.

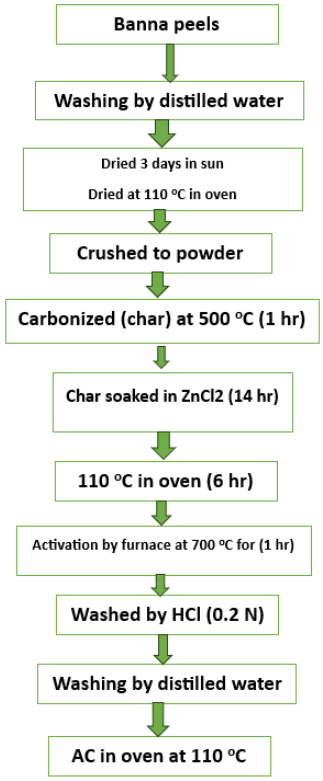

Figure 3. The flow chart regarding the synthesis of ACBP

Table 4. Physical properties of BP and AC

Properties	Banana Peels (before burn)	Activated Carbon (after burn)
Surface area (m^2/g)	7.2016	19.1815
Bulk density (gm/ml)	2.8452	0.4942
Ash content	13.12%	40.49%

Table 5. The GW initial values of anions, cations and TDS compared with FAO

Pollutants	GW of Al-Raeed Research Station	FAO Standard Irrigation Water
EC (µs/cm)	7500	3000
pH	8.2	6-8.5
Pollutants (ppm)		
TDS	5390	2000
Ca	130	400
Mg	200	60
SO_4	1321	960
Cl	990	1065
HCO_3	750	610
CO_3	0	3
K	15.5	2
Na	1200	920
NO_3	10.1	10

Table 4 displays the effects of activated carbon and banana peels. Measurements of the adsorbent's physical properties are detailed in Table 4. The information in the table was gathered from the well irrigation system at the Ministry of Water Resources' Al-Raaed station in Abu Ghraib. The banana peels were synthesized using activated carbon. The initial levels of anions, cations, and TDS in groundwater were compared to FAO standards in Table 5.

3.2 Characterization of ACPB

The (SEM) results were performed for activated banana peels. The functional groups in the raw material (banana peel) were assessed using Fourier Transform Infrared Spectrophotometry (FT-IR) spectra and measured XRD.

4. RESULT AND DISCUSSION

4.1 The effect of dosage

In a 1-hour experiment at room temperature, and pH 8.2, the effect of sorbent dose on ions removal was studied using a range of AC (banana peels) concentrations from 0.5 to 3 g with 200 rpm agitation. Figures 4, 5, and 6 show the outcomes of system. Metal retention has been shown to be directly related to sorbent doses 2.5 g. This value was used as the standard for further experiments. Results were predicted because, for a given initial metal concentration, a larger adsorbent mass yields larger sorption sites or surface area [7].

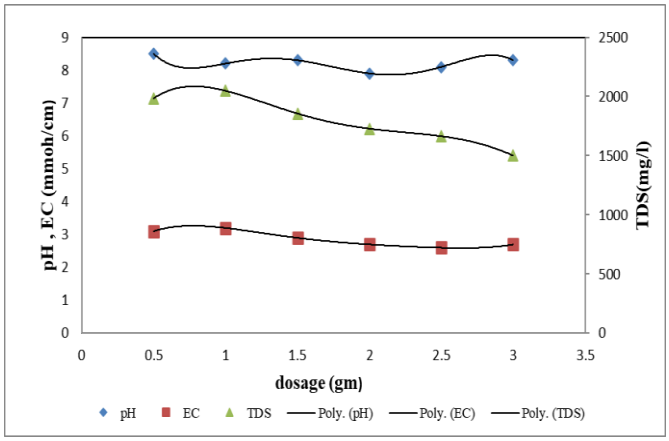

Figure 4. pH, EC, TDS with different dosage (0.5, 1, 1.5, 2, 2.5, 3) gm at (rpm=200, pH=8.2, time=60 min)

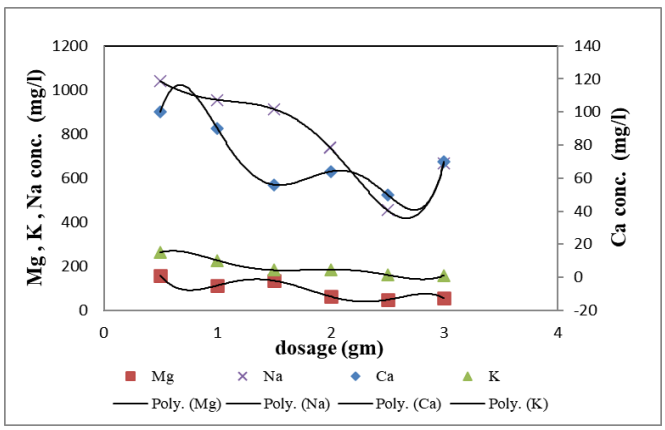

Figure 5. Ca, Mg, K, Na conc. with different dosage (0.5, 1, 1.5, 2, 2.5, 3) gm at (rpm=200, pH=8.2, time=60 min)

Figure 4 depicts the relation between various doses of activated banana peels and the levels of pH, EC, and TDS. The EC exhibited no alteration in its value at different dose levels. The pH value varied with different dosages of BP. The TDS value had a negative correlation with the dosage, as it decreased with increasing dosage. According to the findings, the dose of 2.5 gm was determined to be the most effective in eliminating contaminants from groundwater.

Figure 5 displays the correlation between ion concentrations and dosage. There is a variation in the effectiveness of eliminating contaminants at different dosages of activated banana peels. The removal of contaminants was carried out using 2.5 grams of activated banana peels for sodium (Na) and calcium (Ca) ions. However, for magnesium (Mg) and potassium (K) ions.

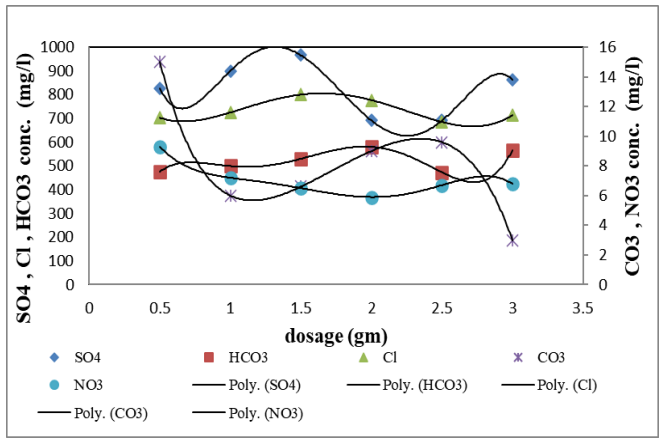

Figure 6. SO_4, Cl, HCO_3, CO_3, NO_3 conc. with different dosage (0.5, 1, 1.5, 2, 2.5, 3) gm at (rpm=200, pH=8.2, time=60 min)

Figure 6 illustrates the association between various doses of activated banana peels and metal ions. Figure 4 illustrates the investigation of the relationship between metal ions at different concentrations. The maximum elimination of contaminants was achieved with a dosage of 2-2.5 grams for SO_4. The maximum elimination of HCO_3 was achieved at a dosage of 2.5 grams. The optimal adsorbent dose for eliminating the pollutant was determined to be 2.5 grams for Cl. The greatest dose for eliminating pollutants in the case of CO_3 was determined to be 3.0 grams.

4.2 The effect of contact time

The duration of contact is crucial for the efficient removal of various ions with BP. The equilibrium time was obtained by examining the adsorption of groundwater at a constant temperature, optimal adsorbent dosage, optimal agitation speed, and optimal pH, as a function of the contact time. This analysis is shown in Figures 7, 8 and 9. The rate of metal removal increases as the contact length increases from 0 to 60 minutes. The absorption rate is governed by the speed at which the adsorbate is transferred from the surface of the particle to its interior sites as the surface sites get exhausted [14, 20].

Figure 7 illustrates the relationship between contact time and the values of pH, EC, and TDS. After 10 minutes, the pH level is 3. The removal of contaminants was shown to be directly proportional to the duration of contact. Conversely, the EC value for contaminated samples was either eliminated or reduced when the contact period was increased to 60 minutes. Through various time intervals, it was determined that a duration of 60 minutes was the most effective in eliminating pollutants.

Figure 8 demonstrates the correlation between the concentrations of metal ions (calcium, magnesium, potassium, and sodium) and the duration of contact. It was demonstrated that prolonging the contact period resulted in the removal of

metal ions. The concentrations of K, Na, Ca, and Mg decreased with increasing contact duration. Therefore, the removal of pollutants was found to be directly proportional to the duration of contact.

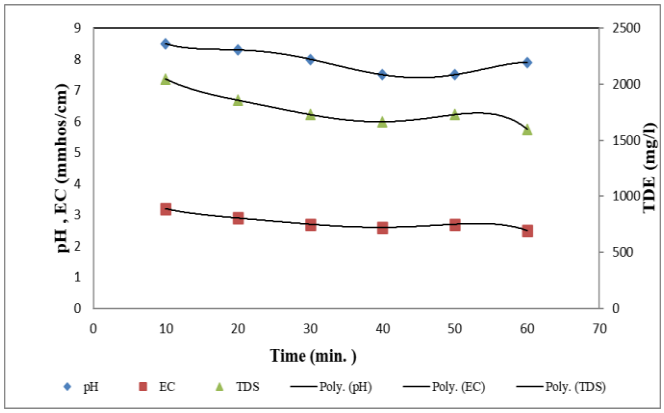

Figure 7. pH, EC, TDS with different time (10, 20, 30, 40, 50, 60) min at (rpm=200, pH=8.5, dosage=2.5 gm)

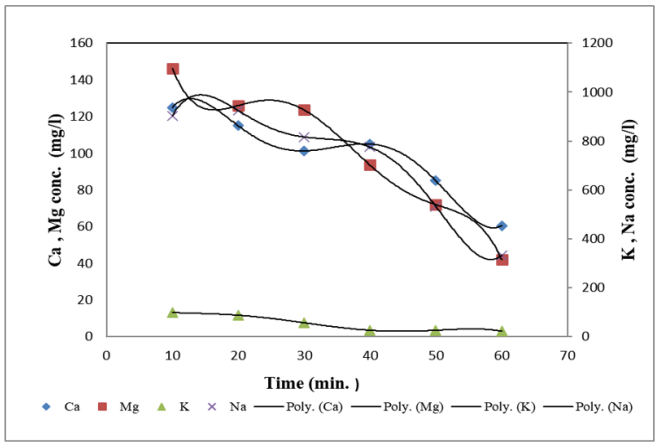

Figure 8. Ca, Mg, K, Na conc. with different time (10, 20, 30, 40, 50, 60) min at (rpm=200, pH=8.5, dosage=2.5 gm)

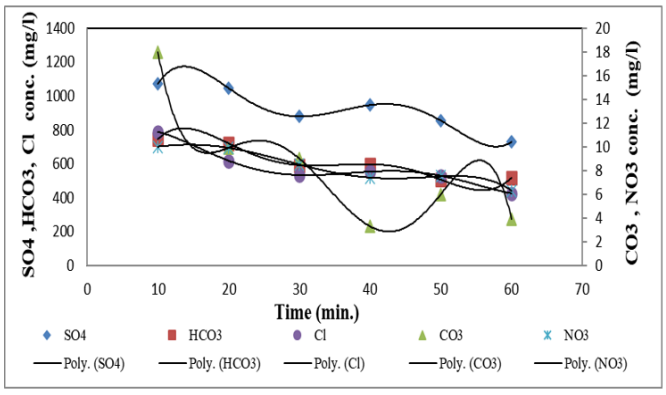

Figure 9. SO_4, HCO_3, CO_3, Cl, NO_3 conc. with different time (10, 20, 30, 40, 50, 60) min at (rpm=200, pH=8.5, dosage=2.5 gm)

Figure 9 illustrates the correlation between the amounts of SO_4, HCO_3, Cl, CO_3, and NO_3. It was stated that prolonging the contact duration resulted in the extraction of ions from groundwater. The ion concentration dropped as the contact time increased. It was determined that a 60-minute duration was the most effective time for eliminating contaminants.

4.3 The effect of agitation speed

Figures 10, 11 and 12 illustrate the impact of different agitation speeds on the removal of all metal ions using the ACBP. Increasing the agitation speed results in a corresponding increase in efficiency values. The thickness of adsorption is increased by raising the agitation speed because the external barrier to mass movement around the adsorbent particles becomes thinner as a result of increased turbulence [21, 22]. The findings also indicate that an agitation speed of 125 rpm is sufficient to achieve optimal clearance by decreasing the thickness of the boundary layer.

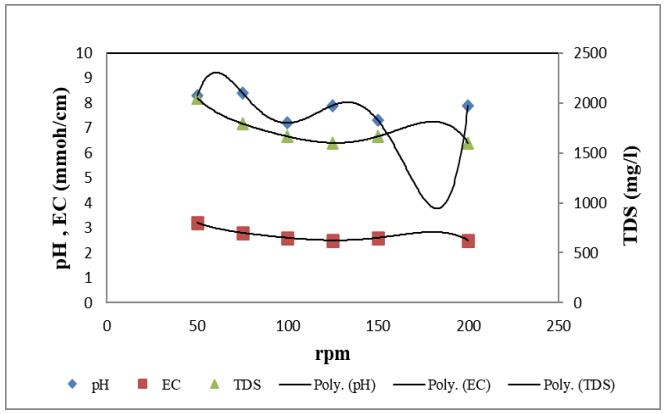

Figure 10. pH, EC, and TDS with different rpm (50, 75, 100, 125, 150, 200) at (time=60, pH=8.2, dosage=2.5 gm)

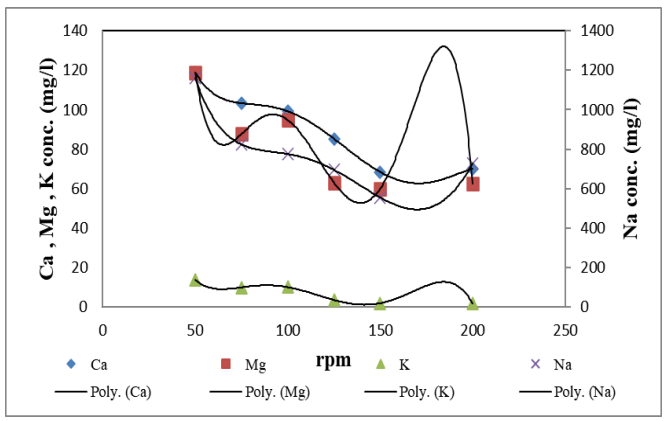

Figure 11. The Ca, Mg, K, Na with different rpm (50, 75, 100, 125, 150, 200) at (time=60, pH=8.2, dosage=2.5 gm)

Figure 10 illustrates the correlation between agitation speed and pH, EC, and TDS, respectively. At a rotational speed of 50 revolutions per minute (rpm), the pH and EC values exhibited a drop. The TDS value was augmented at a speed of 50 rpm and then diminished at a speed of 200 rpm. The total dissolved solids (TDS) exhibited a positive correlation with the rise in the value of revolutions per minute (rpm). The pH value is 9 at a speed of 50 rpm, and 7 at a speed of 100 rpm. At high speeds, the pH value increases and reaches 8 at 200 rpm. The agitation speed affects the parameters of pH, EC, and TDS together.

Figure 11 illustrates the correlation between the concentration of Ca, Mg, K, and Na with the speed of agitation. The agitation speed was found to be inversely proportional to the concentration of metal ions. At a low agitation speed of 50 rpm, the concentration of metal ions exhibited a rise.

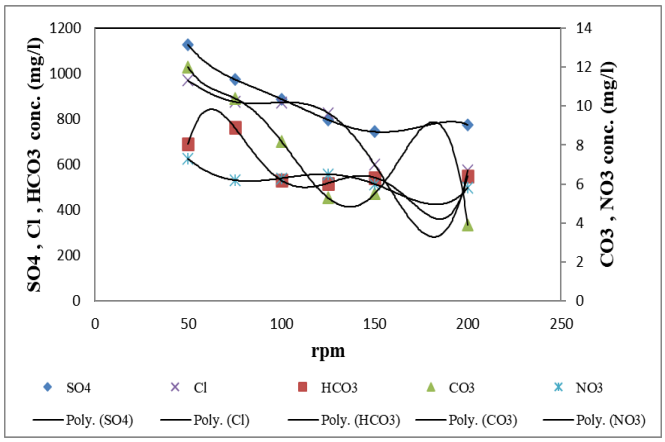

Figure 12. SO_4, CO_3, HCO_3, Cl, NO_3 with different rpm (50, 75, 100, 125, 150, 200) at (time=60, pH=8.2, dosage=2.5 gm)

Figure 12 illustrates the correlation between agitation speed and the concentrations of SO_4, Cl, HCO_3, CO_3, and NO_3 in milligrams per liter (mg/L). The concentration of SO_4 exhibited an upward trend when the agitation speed was set at a low value of 50 rpm. At the greatest level of agitation speed (200 rpm), the values of SO_4, Cl, and HCO_3 declined significantly, indicating a low overall value. Furthermore, the concentration of metal ions such as CO_3 and NO_3 reduced rapidly with increased agitation speed.

4.4 The effect of pH

The influence of pH on the removal efficiency of different metals from a system may be observed in Figures 13, 14, and 15. The adsorption studies were carried out at pH levels that were below 7 to ensure that the results were not affected by the precipitation of metal hydroxides, which occurs at pH values over 7 [23]. At a pH ranging from 2 to 4, the surface of the adsorbent becomes positively charged as it undergoes protonation. This positive charge hinders the entry of metal ions to the adsorbent surface by causing repulsive interactions. At a pH of approximately 5, there is a noticeable increase in the absorption of metals. The presence of a higher number of OH- groups on the surface of an adsorbent results in the surface acquiring a negative charge. The presence of a negative charge on the adsorbent attracts metal ions towards it [22].

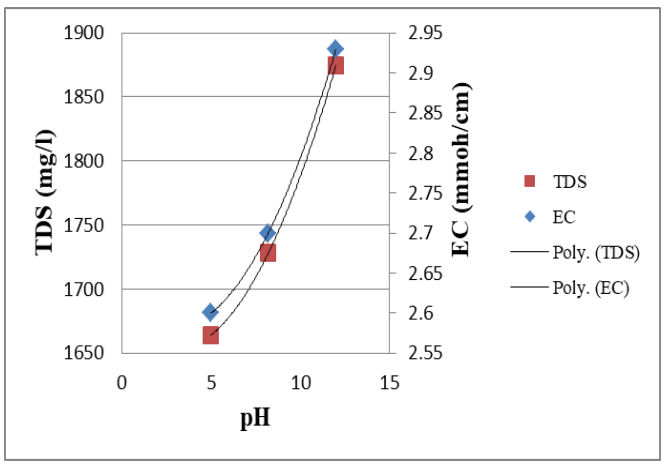

Figure 13. The EC and TDS with different pH, rpm (125) at (time=60, dosage=2.5 gm)

In Figure 13, it showed the relation between pH with TDS and EC. At pH is equal to 5, the value of EC was 2.6 mmoh/cm and the value of TDS was 1664 mg/L. at high value of pH, both the TDS and EC was increased. At the value of pH is equal to 8.2, the value of TDS was 1728 mg/L and the value the EC was 2.7 mmoh/cm in which this value of pH was considered to be the suitable pH value.

In Figure 14, it showed the relation between pH and the metal concentration. At pH value of 5, the value of metal ions was decreased and then became increased with increasing the pH. At pH value was equal to 12, the value of metal concentrations was increased. Thus, the value of pH was equal to 5, is considered to be the suitable value for this study.

In Figure 15, it was shown the relation between metal ions (SO_4, HCO_3, and CI concentration and the pH). The relation is shown that the pH effects the SO_4 ions in which at pH equal to 5, it expressed the decreased pH and it is increased at the highest value of pH. However, the Cl ions expressed lowest value of concentration with increasing pH. The CO_3 and NO_3 showed increasing in pH with increasing concentration. At the lowest pH, the concentration was decreased and at pH equal to 12the concentration in increase. The experiments were performed at dosage equal to 2.5 gm and the time is equal to 60 min with 125 rpm agitation speed.

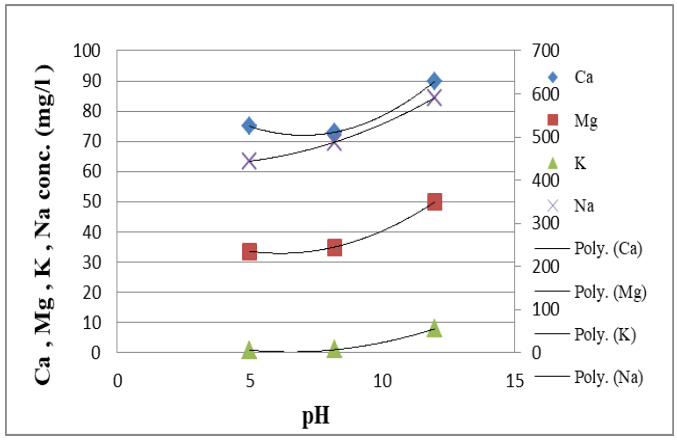

Figure 14. The Ca, Mg, K, Na with different pH, rpm (125) at (time=60, dosage=2.5 gm)

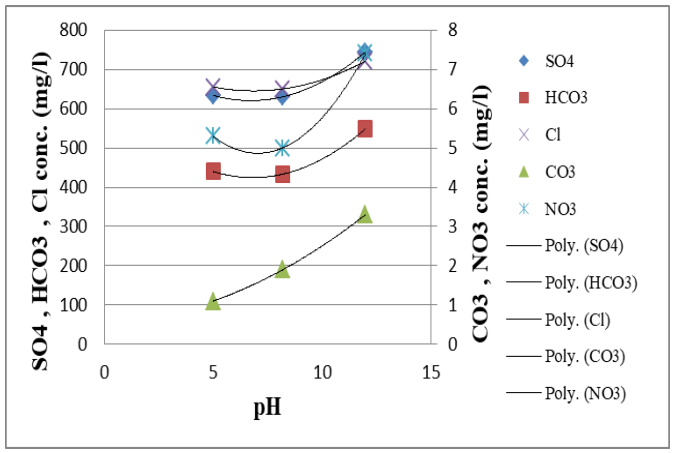

Figure 15. SO_4, CO_3, HCO_3, Cl, NO_3 with different pH, rpm (125) at (time=60, dosage=2.5 gm)

Our findings are in line with those of Naser and Abdul-Hameed [11], who found that OP and chemically modified OP both functions exceptionally well as copper (II) biosorbents,

among the bio-sorbents discussed in earlier studies. The study's key takeaways are: The absorption of copper (II) was shown to be larger at a higher pH. A pH of 7 was the sweet spot when the clearance rate hit 99.6%. Adsorbent dose concentrations of 1g L^{-1} provide the highest removal value. The removal percentage of metal ions is proportional to the agitation speed. The removal rate starts to drop after peaking at 99.63% at 200 RPM. A range of 71.81% to 99.48% of metal ion absorption is observed between 15 and 90 minutes of contact time. It was best to have a 60-minute session. In order to perform the adsorption studies, Cu^{2+} concentrations ranging from 0.5 to 2 mg L^{-1} were utilized. A higher ratio of ion removal is achieved with a lower initial concentration of ions. The highest achievable removal rate was 99.63% at 1 mg L^{-1}.

According to Raheem and Abdul-Hameed [8], the electro-flash reactor technology enhances the potential environmental benefits of using agricultural waste in the flash graphene synthesis process by optimizing the process parameters for producing flash graphene from a variety of carbonaceous materials and efficiently expanding. provides a method for the efficient and cost-effective synthesis of graphene at larger scales.

One of the many potential applications of graphene was in an adsorption batch experiment that used flash graphene to purge anions, cations, and heavy metals from the material in an effort to purify groundwater. We found that banana peels, which are rich in activated carbon, worked just as well as graphene.

Al Haider et al. [7] stated that batch results showed that copper-DPSAC interaction had a substantial impact on pH value, agitation velocity, dosage of activated carbon, balance interaction duration, and copper concentration. These limits were best estimated as 100 minutes, 50 mg/L, 6, 250 rpm, and 3 g/100 mL, respectively, to achieve the highest elimination efficiency of Cu^{+2} (95.542%). Data on copper sorption on DPSAC were in good agreement with Freundlich and Langmuir sorption models. The cop-per migration through the APSAC, however, led to the selection of the Langmuir model with the largest R2. Under equilibrium conditions, a 1D numerical model computed using COMSOL software demonstrated that the DPSAC is a viable method for obstructing the copper plume. The predicted and experimental results, however, are in perfect agreement, with a root-mean-square error (RMSE) of less than 0.1 percent. In order to remove Cu^{+2} from polluted groundwater, the experimental findings showed that DP-SAC were an effective and cost-effective reactive material for the PRB.

Another study performed by Baeza-Serrano et al. [24] utilized metabarcoding to examine the impact of industrial components on microbial populations in four plants exposed to spills: tannery, cannery, textile, and fruit products.

Akter et al. [25] stated that heavy metal concentrations significantly decreased from the river's source to its endpoint, the Buriganga river. While rainwater may have reduced heavy metal concentrations, they still exceeded the allowed amount. Heavy metals, pH, DO, BOD, TDS, TSS, EC, Cl, and Na were identified in surface and groundwater samples above national (DoE) and international (WHO) criteria.

Mahler and Ghimire [26] stated the 35-year longitudinal dataset illuminates state water challenges. Idahoans are satisfied with their drinking water, and voluntary actions to protect water quality (from 12.6% in 1987 to over 63% in 2022) and conserve water quantity (from 16.4% to 64% in 2022). The study acknowledges citizen-led water resource protection and uses this large dataset to influence Idaho water education priorities.

Spengler and Heskett [27] stated that average pharmaceutical and nutrient levels in streams and springs in areas with high OSDS and sewer line densities were slightly higher but not statistically different from those in areas with low densities. Nitrate and silica concentrations in some O'ahu streams and springs are mostly due to sugarcane production on upgradient terrain, not wastewater input. The negligible quantities of pharmaceuticals found in the streams and springs under baseflow conditions show that legacy OSDS and sewage line exfiltration contribute less than 20% of the wastewater flux originally predicted.

4.5 Morphological analysis (SEM)

The surface morphology of the activated carbon samples was examined using scanning electron microscopy (SEM). Scanning electron microscopy (SEM) was used to analyze both the activated banana peel bio-adsorbent and the raw banana peel. The outcomes are shown in Figure 16(a) and Figure 16(b). Distinct disparities in the porosity and surface morphologies of the images were uncovered. The activated banana peel bio-adsorbent appears to possess increased surface area and porosity due to the activation and preparation procedures. The previous study [28] yielded highly similar results, indicating a significant increase in the surface area of the activated adsorbent.

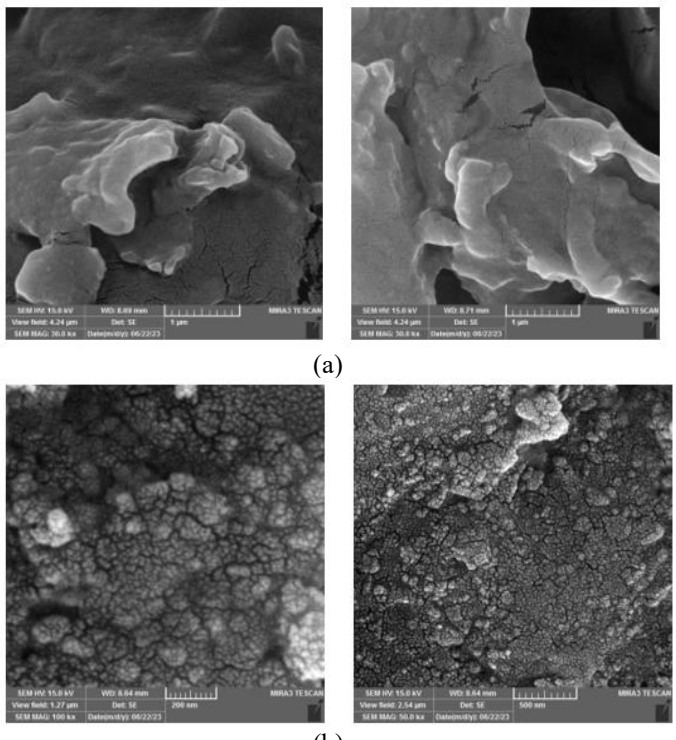

(a)

(b)

Figure 16. (a) SEM for banana peels before burn, (b) SEM for activated carbon (adsorbent) after burn

4.6 Fourier Transform Infrared Spectrophotometer (FT-IR)

Chemical groups present in activated carbon can be determined using Fourier Transform Infrared Spectrophotometer (FTIR) analysis. Various techniques were

employed to analyze and describe the flash graphene forms. Figure 16(a) displays the FTIR spectra of banana peels during the pre-burning phase. The FTIR spectra were obtained in reflectance mode with a resolution of 4 cm^{-1}, covering a spectral range from 4000 to 4500 cm^{-1}. The chemical mechanisms responsible for the adsorption in the spectral range of 2000 to 1000 cm^{-1} were determined. The peak observed at 2000 cm^{-1} is likely attributed to the presence of carbonyl (C=O) groups. The peak at 1000 cm^{-1} can be attributed to polyacrylamide molecules (C-H), while the additional adsorption peak at 3000 cm^{-1} is likely due to the presence of hydroxyl groups. These groups cause the activated carbon structure to be dislodged through vibration.

Figure 17(a) and (b) presents the FTIR spectra of both the activated and inactivated samples of banana peel (BP). In order to gain a deeper understanding of the composition of the functional groups present in banana peels, we obtained Fourier Transform Infrared (FTIR) spectra of BP. The intricate composition of the adsorbent was evidenced by the several peaks detected in the FTIR analysis.

The spectra of (BPAC) exhibit prominent absorption peaks at approximately 3400-3500 cm^{-1}, indicating the presence of carboxylic acid and amino groups. A plausible rationale for the absorption band detected within the range of 2900 to 2970 cm^{-1} is the asymmetrical oscillation of -CH. The observation of stretching vibration bands in the range of 1600-1650 cm^{-1} is due to the asymmetric stretching of the carboxylic C=O double bond. The vibration of carboxylates towards phenolic -OH and -C=O is shown by a spectral peak at 1365-1400 cm^{-1}. The occurrence of prominent peaks in the 832 cm^{-1} range suggests the presence of bioligands27 containing nitrogen. The peaks detected at 1054.40-534.42 cm^{-1} were attributed to Si-O stretching and bending, indicating the presence of silica [29].

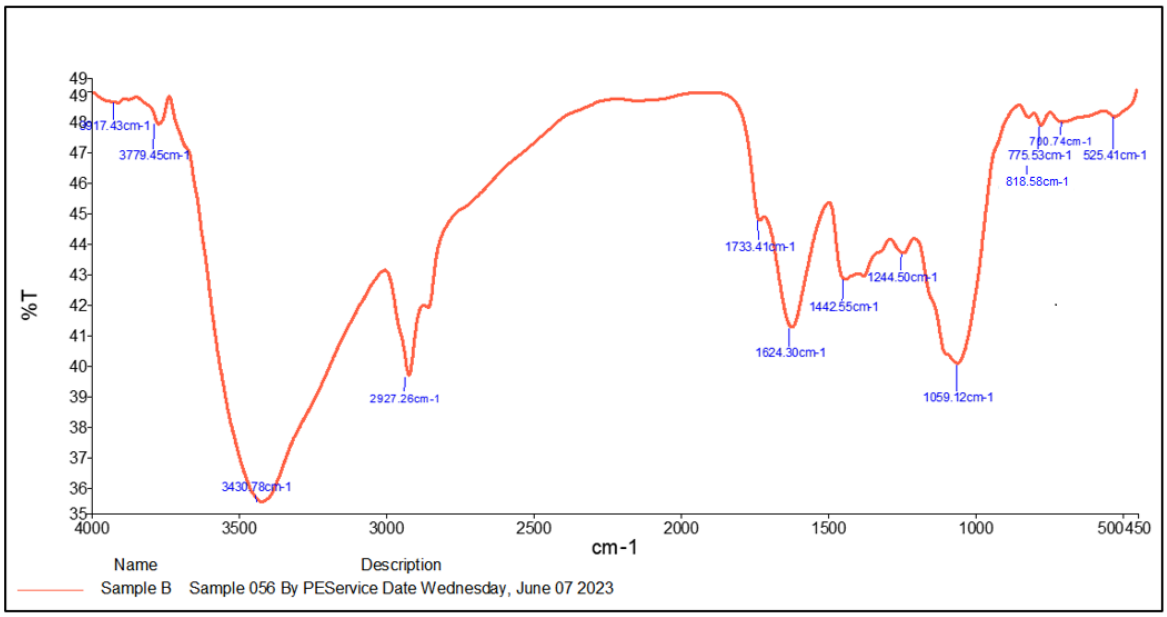

(a)

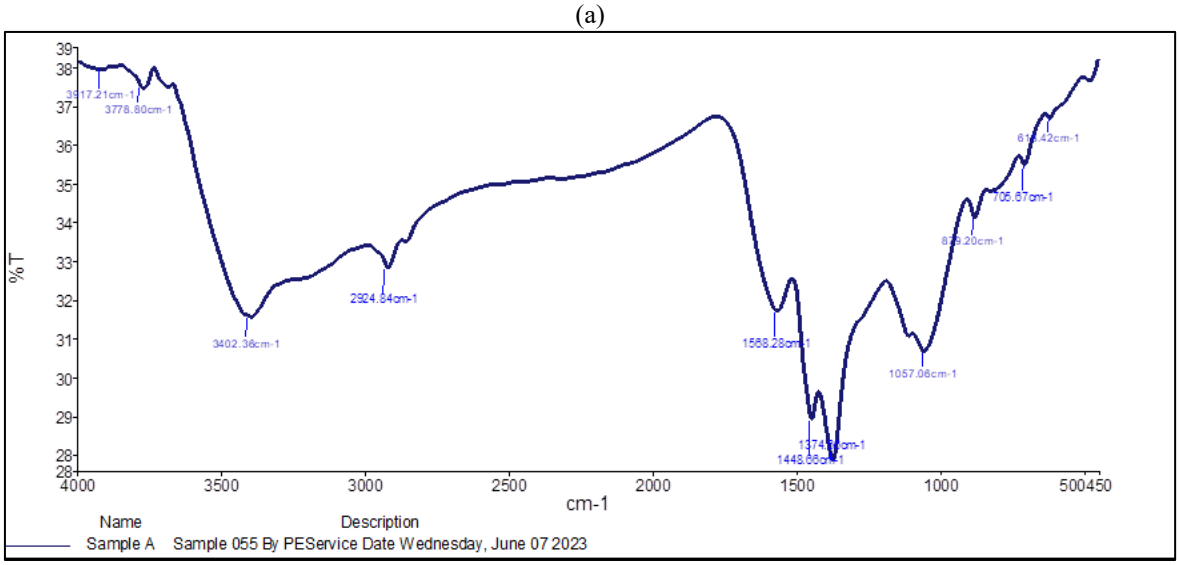

(b)

Figure 17. (a) The FTIR of banana peel before burning, (b) The FTIR of banana peel (activated carbon) after burning

Maharjan and Jha [17] illustrated in the synthesis of AC that Activated BP lost some functional groups during heat treatment, which may be because of the existence of a high number of micropores, as shown by the discrepancy between the FTIR spectra of raw and activated banana peels. By increasing the number of pores between carbon atoms, the carbonization and activation processes remove less stable volatile materials in the form of fumes made of oxygen

derivatives. Therefore, a more precise distribution of pore sizes is possible by physical activation.

4.7 The XRD (X-ray diffraction)

X-ray diffraction (XRD) was used to investigate the structural investigation of carbonaceous materials. The X-ray diffraction (XRD) data in Figure 18(A) and (B) were compared to the graphite ICSD card 31170, which has a space-group of P63mc. The samples exhibit diffraction peaks at lower activation temperatures (250℃ and 300℃) that do not correspond to the patterns in the ICSD card [30, 31]. The diffraction peaks found in Figure 16 are present at lower carbonization temperatures (300℃). The samples exhibit significantly widened (002) and (012) peaks at around 25 and 40 position (θ0), indicating a substantial level of disorder in the samples. This suggests a greater presence of amorphous carbon in all of the samples. Figure 16 depicts two components: (A) represents banana peels prior to combustion, whereas (B) represents the activated carbon derived from burned banana peels [32].

Figure 18 displays the XRD patterns of physically stimulated banana peels. The X-ray diffraction (XRD) profiles of pyrolytic banana peels displayed distinct peaks, suggesting alterations in the activated carbon's structure. It has been verified that when activated banana peel carbon is subjected to a pyrolysis temperature of 300℃, it undergoes thermal decomposition and transforms into a crystalline graphitic form of carbon, with chaoite peaks observed at 28.6° and 31.7° (and further peaks at 24.5° and 30°) [33].

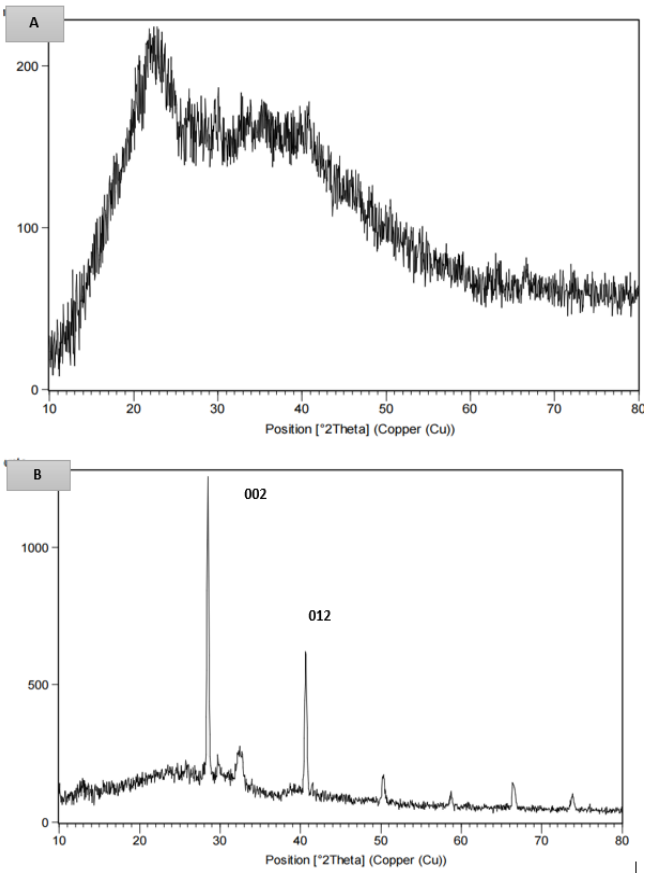

Figure 18. The XRD diffraction spectra of activated carbon banana peel samples (ACBP) (A) before burning, and (B) after burning

The peak observed at an angle of 66.60° was identified as alumina, whereas the peak at 73.9° was identified as silicon dioxide [33]. Figure 18 displays the X-ray diffraction (XRD) patterns of both Banana peel and its activated carbon produced under different conditions.

The XRD patterns indicated that the pyrolytic products were not completely pure and contained some impurities. The impurities present in the sample consist of amorphous carbon (specifically activated carbon) at a temperature of 59°, Fe_3C at 40.8°, Fe_2O_3 at 34.5º, and K_2O at 50.5°. It indicates that the pyrolysis reaction was incomplete and amorphous carbon remained. It was hypothesized that Fe metal separated from banana peels and underwent dissociation to react with carbon and oxygen, forming Fe_3C and Fe_2O_3. Regarding K_2O, the high potassium level in banana peels caused it to react with oxygen during the oxidation reaction [34, 35]. According to Figure 18, the intensity of the peak for activated carbon is greater for physically activated banana peels compared to raw banana peels. This increased intensity results in a higher adsorption capacity. The prominent X-ray diffraction (XRD) peaks shown in Figure 18(B) can be attributed to the enhanced porosity structure of banana peels following activation, as compared to their raw state.

Maharjan and Jha [17] stated in the synthesis of AC that in comparison to raw banana peels, physically activated banana peels have a much stronger peak for activated carbon, indicating that they have a higher adsorption capability. The increase in the porosity structure of banana peels after activation compared to raw banana peels is the reason behind the high intensity XRD peaks of physically activated carbon.

5. CONCLUSIONS

Groundwater is an important source for a drink and irrigation at Al-Raaed station in Abu Ghraib affiliated to the Ministry of Water Resources. In this research, four parameters studied in adsorption process (dosage, time, agitation speed and pH) to know the best terms that used to get groundwater suitable for irrigation. Understanding knowledge of irrigation water quality is critical to the management of water for long-term productivity. Water samples were analyzed in a laboratory for some of the key quality indicators; pH, EC, total dissolved solid (TDS), Ca, Mg, Na, K, CO_3, HCO_3, SO_4, Cl, NO_3, etc. The overall objective of this study was to use groundwater for irrigation of agricultural crops. The removal efficiency at 2.5 g was the best (57%), (76%), (94%) for Ca, Mg and K respectively. for the time, the optimum time is 60 min. The removal efficiency was (53%), (79%), (57%) for Ca, Mg and Cl respectively. Regarding to agitation speed the best option is located at 150 rpm, the removal efficiency is (47%) for Ca, (53%) for Na and (40%) for NO_3 and (39%) for Cl. When changing pH, the approaching from 7 is the best, the removal efficiency is (83%) for Mg, (52%) for SO_4, (94%) for K and (63%) for Na.

1. The removal efficiency of activated banana peels for the $Ca^{2+} < Cl^{1-} < Mg^{2+}$ ions.

2. The FTIR examination revealed the presence of several types of groups, with the hydroxyl and carbonyl groups shifting to a lower frequency and thereby playing the most crucial role in the adsorption of Ca^{2+}, Mg^{2+}, and $SO4^{-2}$, correspondingly.

3. For overall metals, the optimal pH, agitation speed, adsorbent dose, and contact duration were 5, 150 rpm, 2.5 g,

and 60 min, correspondingly.

To completely understand the environmental impacts of larger-scale activated carbon, more research is needed. Academic and commercial institutions should conduct more in-depth studies on the stability and degradation of larger-scale activated carbon synthesis in response to the material's increasing demand using different natural biowaste as an adsorbent material.

Future research could expand the parameters explored in this study to include more variables, such as temperature and additional pH values, that improve the remediation processes for GW and wastewater, which can then be used for irrigation.

In order to remove inorganic such as heavy metals from polluted groundwater, the experimental findings will be investigated and show whether that ACBP were an effective and cost-effective reactive material for the PRB. More experimental works were needed to investigate the sustainability of using activated carbon from banana peels and its advantages over conventional methods. The potential for scaling up the production and use of banana peel activated carbon and its integration into existing water treatment systems will be considered as a new future works should be performed.

REFERENCES

[1] Acharya, S., Sharma, S.K. (2016). Groundwater assessment and its electrochemical treatment. International Journal of Advanced Technology in Engineering and Science, 4(3): 21-30.

[2] Achmad Chafidz, W., Astuti, D., Hartanto, A., Septiani, A., Mutia, P.R., Sari, P.R. (2018). Preparation of activated carbon from banana peel waste for reducing air pollutant from motorcycle muffler. MATEC Web of Conferences, 154: 01021. https://doi.org/10.1051/matecconf/201815401021

[3] Wu, J., Li, P., Qian, H., Fang, Y. (2014). Assessment of soil salinization based on a low-cost method and its influencing factors in a semi-arid agricultural area, northwest China. Environmental Earth Sciences, 71(8): 3465-3475. https://doi.org/10.1007/s12665-013-2736-x

[4] Wu, J., Sun, Z. (2016). Evaluation of shallow groundwater contamination and associated human health risk in an alluvial plain impacted by agricultural and industrial activities, mid-west China. Exposure and Health, 8: 311-329. https://doi.org/10.1007/s12403-015-0170-x

[5] Malakootian, M., Yousefi, N. (2009). The efficiency of electrocoagulation process using aluminum electrodes in removal of hardness from water. Iranian Journal of Environmental Health Science and Engineering, 6(2): 131-136.

[6] Jasim, N., Ebrahim, S., Ammar, S. (2023). Fabrication of ZnxMn1-xFe2O4 metal ferrites for boosted photocatalytic degradation of Rhodamine-B dye. Results in Optics, 13: 100508. https://doi.org/10.1016/j.rio.2023.100508

[7] Al Haider, S., Al Fatlawi, S., Nasir, M. (2021). Utilizing activated carbon developed from banana peels as permeable reactive barrier in copper removal from polluted groundwater. Journal of Ecological Engineering, 23(1): 83-90. https://doi.org/10.12911/22998993/143973

[8] Raheem, N., Abdul-Hameed, H. (2024). Groundwater remediation using flash graphene produced from banana peels: Batch mode. International Journal of Environmental Impacts, 7(2): 319-327. https://doi.org/10.18280/ijei.070216

[9] Al-Sareji, O.J., Grmasha, R.A., Meiczinger, M., Al-Juboori, R.A., Somogyi, V., Hashim, K.S.A. (2024). Sustainable banana peel activated carbon for removing pharmaceutical pollutants from different waters: Production, characterization, and application. Materials, 17: 1032. https://doi.org/10.3390/ma17051032

[10] Ali, A., Elwardany, R., Mustafa, A., Shokry, H. (2024). Remediation of contaminated water using cellulose acetate membrane hybrid by sunflower seed shell-activated carbon. Biomass Conversion and Biorefinery, 1-17. https://doi.org/10.1007/s13399-024-05326-6

[11] Naser, Z.A., Abdul-Hameed, H.M. (2022). Removal of Cu (II) from industrial wastewaters through locally-produced adsorbent prepared from orange peel. Caspian Journal of Environmental Sciences, 20(1): 45-53. https://doi.org/10.22124/cjes.2022.5391

[12] Çadraku, H.S. (2021). Groundwater quality assessment for irrigation: Case study in the Blinaja River Basin, Kosovo. Civil Engineering Journal, 7(9): 1515-1528. https://doi.org/10.28991/cej-2021-03091740

[13] Wu, J., Zhang, Y., Zhou, H. (2020). Groundwater chemistry and groundwater quality index incorporating health risk weighting in Dingbian County, Ordos basin of northwest China. Geochemistry, 80(4): 125607. https://doi.org/10.1016/j.chemer.2020.125607

[14] Gayathiri, M., Thiruchelvi, P., Kumar, K.T.L., Kumar, S. (2022). Activated carbon from biomass waste precursors: Factors affecting production and adsorption mechanism. Chemosphere, 294: 133764. https://doi.org/10.1016/j.chemosphere.2022.133764

[15] Jasim, N., Ebrahim, S., Ammar, S. (2023). A comprehensive review on photocatalytic degradation of organic pollutants and microbial inactivation using Ag/AgVO3 with metal ferrites based on magnetic nanocomposites. Cogent Engineering, 10(1): 2228069. https://doi.org/10.1080/23311916.2023.2228069

[16] Van Loon, J.C. (1985). Chemical analysis of inorganic constituents of water. CRC Press, Boca Raton.

[17] Maharjan, J., Jha, V.K. (2022). Activated carbon obtained from banana peels for the removal of As (III) from water. Scientific World, 15(15): 145-157. https://doi.org/10.3126/sw.v15i15.45665

[18] Iftekhar, S. (2018). Understanding the factors affecting the adsorption of lanthanum using different adsorbents: A critical review. Chemosphere, 204: 413-430. https://doi.org/10.1016/j.chemosphere.2018.04.067

[19] Müller, B.R. (2010). Effect of particle size and surface area on the adsorption of albumin-bonded bilirubin on activated carbon. Carbon, 48: 3607-3615. https://doi.org/10.1016/j.carbon.2010.06.011

[20] Nadew, T.T., Keana, M., Sisay, T., Getye, B., Habtu, N.G. (2023). Synthesis of activated carbon from banana peels for dye removal of an aqueous solution in textile industries: Optimization, kinetics, and isotherm aspect. Water Practice & Technology, 18(4): 947. https://doi.org/10.2166/wpt.2023.042s

[21] Ramutshatsha-Makhwedzha, D., Mavhungu, A., Moropeng, M.L., Mbaya, R. (2022). Activated carbon derived from waste orange and lemon peels for the adsorption of methyl orange and methylene blue dyes

from wastewater. Heliyon, 8: e09930. https://doi.org/10.1016/j.heliyon.2022.e09930
[22] Wei, J. (2018). Experimental and theoretical investigations on Se (IV) and Se (VI) adsorption to UiO-66-based metal-organic frameworks. Environmental Science: Nano, 5(6): 1441-1453. https://doi.org/10.1039/C8EN00282H.
[23] Çelebi, H., Gök, G., Gök, O. (2020). Adsorption capability of brewed tea waste in waters containing toxic lead (II), cadmium (II), nickel (II), and zinc (II) heavy metal ions. Scientific Reports, 10(1): 17570. https://doi.org/10.1038/s41598-020-74553-4
[24] Baeza-Serrano, Á., Oliver, N., Sempere, F., Montoya, T. (2023). Microbial community of activated sludge in four wastewater treatment plants affected by industrial spills. International Journal of Environmental Impacts, 6(2): 81-87. https://doi.org/10.18280/ijei.060204
[25] Akter, A., Hossain, M., Khan, R.A., Faiz, S.M.A. (2023). Effects of tanning on seasonal variation in the physiochemical quality of surface and groundwater and including an analysis of trace metals in Hazaribagh. International Journal of Environmental Impacts, 6(2): 73-79. https://doi.org/10.18280/ijei.060203
[26] Mahler, R.L., Ghimire, N. (2023). Public perceptions and responses to water resource issues over the last 35 years in Idaho, USA. International Journal of Environmental Impacts, 6(2): 65-72. https://doi.org/10.18280/ijei.060202
[27] Spengler, S., Heskett, M. (2023). Impact to stream water quality from sewage exfiltration and legacy On-Site Disposal Systems on the island of O'Ahu, Hawaii. International Journal of Environmental Impacts, 6(1): 13-23. https://doi.org/10.18280/ijei.060103
[28] Van Weert, F., Van der Gun, J., Reckman, J.W.T.M. (2009). Global overview of saline groundwater occurrence and genesis. International Groundwater Resources Assessment Centre, 104.
[29] Karić, N., Maia, A.L., Teodorović, A., Atanasova, N., Langergraber, G., Crini, G., Ribeiro, A., Đolić, M. (2021). Bio-waste valorisation: Agricultural wastes as biosorbents for removal of (in) organic pollutants in wastewater treatment. Chemical Engineering Journal Advances, 8: 100239. https://doi.org/10.1016/j.ceja.2021.100239
[30] Fasakin, O., Dangbegnon, J.K., Momodu, D.Y., Madito, M.J., Oyedotun, K.O., Eleruja, M.A., Manyala, N. (2018). Synthesis and characterization of porous carbon derived from activated banana peels with hierarchical porosity for improved electrochemical performance. Electrochimica Acta, 262: 187-196. https://doi.org/10.1016/j.electacta.2018.01.028
[31] Al-Mahmoud, S.M. (2019). Adsorption of some aliphatic dicarboxylic acids on zinc oxide: A kinetic and thermodynamic study. Baghdad Science Journal, 16(4): 0892. http://doi.org/10.21123/bsj.2019.16.4.0892
[32] Alshabander, B., Abd-Alkader, M.B. (2023). Photocatalytic degradation of methyl blue by TiO_2 nanoparticles incorporated in cement. Iraqi Journal of Physics, 21(1): 10-12. http://doi.org/10.30723/ijp.v21i1.1042
[33] Farhan, A.M., Zaghair, A.M., Abdullah, H.I. (2022). Adsorption study of Rhodamine-B dye on plant (Citrus leaves). Baghdad Science Journal, 19(4): 0838. http://doi.org/10.21123/bsj.2022.19.4.0838
[34] Mohamed, S., Kareem, N. (2018). Optical properties for prepared polyvinyl alcohol/polyaniline/ZnO nanocomposites. Iraqi Journal of Physics, 16(36): 181-189. http://doi.org/10.20723/ijp.16.36.181-189
[35] Swady, E.A., Jawad, M.K. (2021). Study FTIR and AC conductivity of nanocomposite electrolytes. Iraqi Journal of Physics, 19(51): 15-22. http://doi.org/10.30723/ijp.v19i51.689